First International Conference on Damage Tolerance of Aircraft Structures
R. Benedictus, J. Schijve, R.C. Alderliesten, J.J. Homan (Eds.)

WELD RESIDUAL STRESS EFFECTS ON FATIGUE CRACK GROWTH BEHAVIOUR OF ALUMINIUM ALLOY 2024-T3

C.D.M. Liljedahl*, J. Brouard†, O. Zanellato*, J. Lin†, J.F. Tan*, S. Ganguly*, P.E. Irving†, M.E. Fitzpatrick*, X. Zhang† and L. Edwards*[1]

*Department of Materials Engineering, The Open University, Milton Keynes, MK7 6AA, UK
e-mail: d.liljedahl@open.ac.uk

†Damage Tolerance Group, Cranfield University, Bedfordshire, MK43 0AL, UK

Abstract. *The interaction between residual stress and fatigue crack growth rate (FCGR) has been investigated in M(T) and CT specimens machined from Variable Polarity Plasma Arc (VPPA) welded Al-2024 plate. The residual stresses were measured with neutron diffraction and the crack closure was continuously monitored using an eddy current transducer located at the crack mouth of the specimens. The effect of the residual stresses on the FCGR was predicted for both specimen geometries using both a residual stress and a crack closure approach. Good correlation was found between the experimental data and both sets of predictions. The initial residual stresses were found to re-distribute with crack growth and the distributions were very different in the M(T) and CT specimens. In particular, the residual stresses accelerated the FCGR in the M(T) specimen whereas it decelerated the growth rate in the CT sample demonstrating the importance of accurately evaluating the residual stresses in welded specimens which will be used to produce damage tolerance design data.*

Keywords: *Residual stress; damage tolerance; neutron diffraction; finite element analysis; eigenstrain; fatigue crack growth; crack closure*

1 INTRODUCTION

Present innovations in aircraft manufacture include the creation of integral structures via manufacturing processes such as welding, rather than traditional riveting [1], so permitting modular pre-fabrication of large integral sections of aircraft prior to final assembly. However, an inherent inconvenience is the residual stress field caused by the welding process, which significantly influences the fatigue life of the structure [2, 3]. Thus, the weld residual stresses must firstly be determined and their effect on fatigue crack growth rate (FCGR) accurately modelled if damage tolerant structures are to be optimally designed [4].

Previous research [5] directly measured changes in fatigue crack closure as the fatigue crack traversed the weld at a constant ΔK, and successfully predicted changes in fatigue crack growth rates using ΔK_{eff} derived from the crack closure measurements. This paper summarises a recent study of weld residual stresses and their redistribution arising from fatigue crack growth [6, 7, 8]. The stresses were directly measured using neutron diffraction, and the data

[1] Currently at the Australian Nuclear Science and Technology Organisation, PMB1, Menai, NSW 2234, Australia.

was used to calculate values of residual stress intensity factors (K_{resid}). In turn this was used as input to the AFGROW model for crack growth rates calculation. The results of this and the experimental closure based model are compared.

In both the M(T) and CT specimens here studied the increased compliance and crack tip plasticity associated with fatigue crack growth cause the local weld residual stress field to relax and redistribute. To study this process a fatigue crack was grown in-situ in the ENGIN-X neutron diffractometer at ISIS, the UK pulsed neutron source [9], and changes in residual stress field arising from crack growth, recorded [6, 7]. The re-distribution of the residual stresses with crack extension was also modelled using finite element analysis. As reported in [5] crack closure was continuously monitored during fatigue crack growth through the weld using an eddy current transducer located at the crack mouth. The effect of residual stresses on the R-ratio (K_{min}/K_{max}) was computed for both specimen geometries using the residual stress (K_{resid}) approach. This was then used to predict the FCGR using an empirical fatigue crack growth law. The predictions were compared with those of the ΔK_{eff} approach reported in Brouard et al. [5].

2 EXPERIMENTAL PROCEDURES AND RESULTS

Single pass autogenous Variable Polarity Plasma Arc (VPPA) welding was used to manufacture 2024 aluminium plates measuring 500×500 mm^2. The plates were welded with the weld direction parallel to the plate longitudinal orientation. An M(T) specimen was machined with the dimensions and orientations shown in Figure 1. The CT sample (Figure 1) was then sectioned from the M(T) specimen using EDM (Electron Discharge Machining).

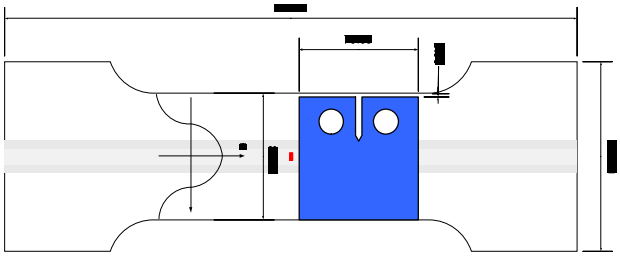

Figure 1: Geometry for the M(T) and CT specimens (the grey regions represent the weld bead).

Samples were subjected to Mode I fatigue loading at constant ΔK and R-ratio of 0.1. Fatigue crack growth rates were measured for the M(T) specimen at a constant ΔK of 6, 11 and 15 MPa√m (see Figure 2). For convenience the predictions are included in those and the subsequent figures. However the modelling work will be discussed later in this paper. It can be seen that the FCGR in the welded specimen is significantly higher than that in the parent material at ΔK of 6 and 11 MPa√m. However, at a ΔK of 15 MPa√m the FCGR is close to the rate in the parent material. The CT specimens were first tested at ΔK of 11 MPa√m but crack arrest occurred as the crack approached the weld line. The load was therefore increased to ΔK =13 MPa√m and the crack grew slowly before crack arrest occurred again. The applied stress

intensity range was then increased further to 15 MPa√m and the crack then grew through the entire specimen. The measured FCGR in the CT specimens are shown in Figure 3a. It can be seen that the rate in the CT specimen tested at ΔK of 15 MPa√m is even lower than the rate in the M(T) specimen tested at ΔK of 6 MPa√m.

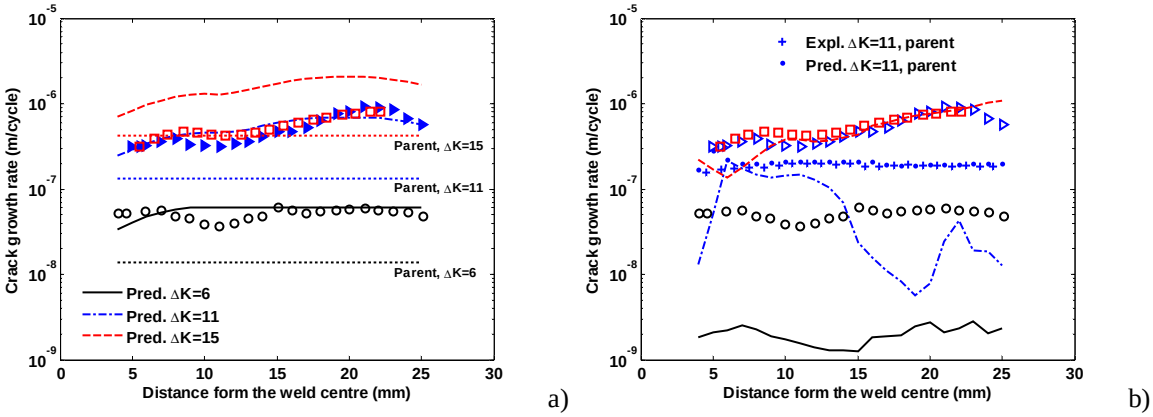

Figure 2 Experimental results and predictions of the crack growth rate in the welded M(T) specimen (applied load: R=0.1, ○-ΔK=6,▶- ΔK=11,□- ΔK=13) a) Using the residual stress approach b) Using the crack closure approach

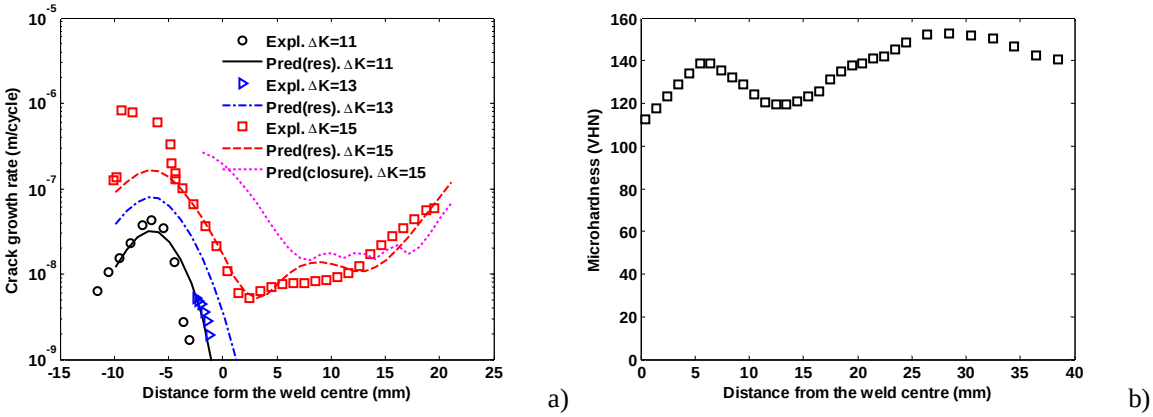

Figure 3 a) Experimental and numerical results of the crack growth rate in the CT specimen (R=0.1, res – predictions using the residual stress approach, closure – predictions using the crack closure approach) b) Micro-hardness measured across the weld and the parent material with a Vickers indenter

The micro-structural hardness profile was also measured, and as shown in Figure 3b. The data suggest that there are significant changes in the microstructure of the material in the transition between the weld centre, the HAZ (heat affected zone) and the parent material.

2.1 Residual stress measurements

Neutron diffraction is an established non-destructive technique to determine stresses within metallic aerospace structures [4]. The measurements were carried out on the ENGIN-X

diffractometer [9], which is based at the pulsed neutron source ISIS, of the Rutherford Appleton Laboratory in the UK. There were two detector banks at ±90º to the incident beam, which allows for measurements in two directions at the same time. Details of these experiments are published elsewhere [6, 7] and for brevity only the results at two typical crack lengths are shown here. The gauge volume used was 2×8×2mm with the longer dimension being oriented so as to sample all the thickness direction of the plate. Plane stress was assumed and hence, only the components in the longitudinal and transverse directions were needed to be determined for computation of the residual stresses. Only the longitudinal stresses are presented here.

In-situ fatigue loading was carried out using a 100kN INSTRON hydraulic test machine. Crack growth rate was measured at a constant ΔK of 6 MPa√m for the M(T) specimen and 17 MPa√m for the CT specimen at R-ratio of 0.1. Measurements were taken as the crack grew from the weld centre (Figure 1) until a half crack length of 25 mm was reached for the M(T) specimen and 44.5 mm for the CT specimen.

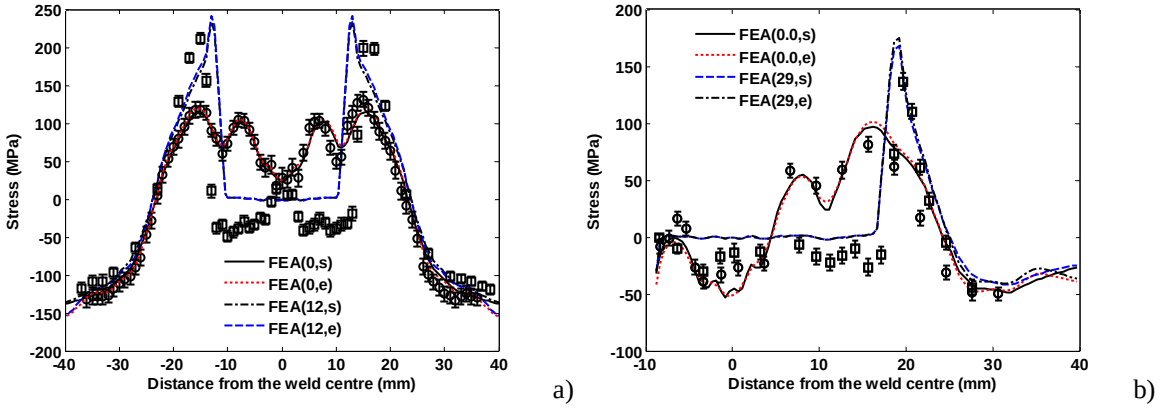

Figure 4 Experimentally determined and predicted residual stresses in the longitudinal direction (s – using the SIGINI subroutine and e – using the eigen-strain approach) a) in the M(T) specimen in unfatigued condition (○) and after 12 mm (□) crack growth and b) in the CT specimen in unfatigued condition (○) and at 29 mm (□) fatigued crack length

The measured residual stresses in the M(T) specimen for the un-fatigued crack free condition and at a crack length of 12 mm are shown in Figure 4a. It can be seen that the residual stresses re-distribute as a result of this crack growth. This was accompanied by an observed increase in crack growth rate in the MT specimen. Measurements were also made at the minimum and maximum loads in the fatigue cycle for some crack lengths and these measurements showed [6] that the measured compressive residual stress field in the wake of the crack for the M(T) specimen (Figure 4a) was independent of applied load and so cannot be due to physical crack closure. Tsakalakos et al. [10] and Croft et al. [11] have measured the residual strain within a single overloaded CT specimen using energy dispersive synchrotron X-ray diffraction. They also found an apparent compressive stress in the wake of the crack even after the specimen was completely fractured; hence again there is no physical closure. Compressive macro-stresses can be ruled out as the crack plane must be a traction-free

surface. These authors suggested that these apparent stresses may be due to anisotropic plastic strains in the crack wake [11] or measurement error due to the gauge volume differing in the two measured directions [10].

The residual stress distribution in the CT specimen in the un-fatigued condition and after a 29 mm of fatigue crack growth is shown in Figure 4b. The initial residual stresses can be seen to be significantly smaller than that observed in the M(T) specimen. Furthermore, it can be seen that due to the notch machined into this specimen the stress field is asymmetric and, in contrast to the MT results, the (compressive) residual stresses near the initial crack tip were little affected by crack growth until the crack tip had grown through the initial compressive residual stress field at about 10 mm from the weld centre.

2.2 Crack closure measurements

Additional tests were carried out on samples where the crack opening load was constantly monitored with an eddy current transducer. The opening stress intensity factor (K_{op}) for the MT and CT is shown in Figure 5. The result for the parent plate of 2024 tested at ΔK=11 MPa√m is also shown.

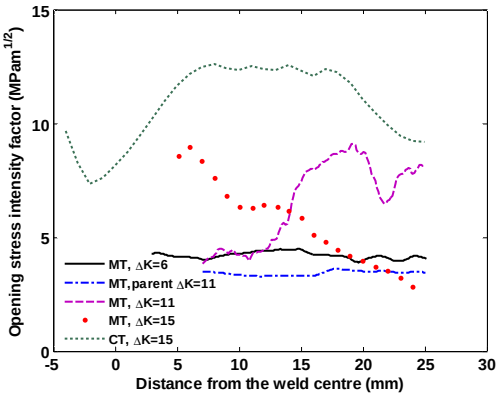

Figure 5 The crack opening stress intensity factor for M(T) and CT specimen (R=0.1)

It can be seen that the crack opening stress intensity factor is constant for the M(T) specimen tested at a ΔK = 6 MPa√m whereas it fluctuates significantly for another M(T) specimen tested at a ΔK = 11 MPa√m. It can also be seen that the crack opening K values are greater than that of the parent material for the latter specimen. This is not consistent with the observed crack growth rates where the rate in the welded sample was faster than in the parent plate (Figure 2b). For the MT specimen tested at ΔK = 15 MPa√m, the K_{op} decreased with crack length. This is reflected in the FCGR for this specimen (Figure 2b). For the CT specimen, a larger crack opening stress intensity factor was seen. This is consistent with the low FCGR found in the specimen tested at a ΔK = 15 MPa√m and the crack arrest that occurred for the specimen tested at low loads.

3 RESIDUAL STRESS EVOLUTION MODELLING

The commercial code ABAQUS (standard version 6.5) was used for all the FE modelling. The plate was thin compared to the width and the gauge volume extended through the whole thickness, so plane stress condition was assumed. Plane stress, 8 noded elements (CPS8) with full integration was used through out this paper. The smallest elements along the crack plane were 0.125 mm^2. A convergence study was undertaken and the results were seen to have converged at this mesh density. For the M(T) specimen only a quarter of the sample was modelled due to double symmetry and half the sample modelled for the CT specimen. An analytical surface and contact elements were assigned along the symmetry lines to avoid surface overlap.

Two approaches were employed to introduce the measured residual stresses in the M(T) sample FE models. The first is the eigenstrain approach [12]. Eigenstrain (ε^*) is a non-uniform inelastic strain which causes elastic strains and hence stresses. Where the residual stresses are known throughout the whole component, then ε^* can be determined from the following relation directly:

$$\varepsilon^* = -C_{ijkl}^{-1}\sigma_{kl}^{RS} \tag{2}$$

where C is the elastic constants tensor and σ^{RS} are the measured residual stresses.

The stress distribution away from the notch was measured in the MT specimen before it was fatigued. This stress distribution was assumed to represent the distribution throughout the un-cracked specimen (i.e. assuming that the welded plate was continuously processed). In this case for a continuously processed body and 2D only one eigenstrain component in the longitudinal direction will contribute to the residual stresses [13] as the other components satisfy the compatibility equation. The transverse stress will also be small in the un-cracked component. The eigenstrain was hence computed as follows:

$$\varepsilon_{11}{}^*(y) = -\frac{\sigma_{11}^{RS}(x)}{E} \tag{3}$$

where E is Young's modulus for the material. The eigenstrain field was introduced into the FEA model using a pseudo anisotropic thermal strain.

As a comparison, the residual stress field was read in directly into the model using the SIGINI FORTRAN subroutine [14]. This is the second approach for modelling the residual stresses distribution. In the first analysis step the stresses were allowed to equilibrate simulating the residual stresses in the M(T) specimen.

The resulting residual stresses using both the SIGINI subroutine and the eigenstrain approaches are shown in Figure 4a. There is a good correlation between the two sets of FE results and the measured data, which also indicates that the measured residual stresses were balanced.

The resulting elastic strain distribution in the CT specimen is compared with the experimental results in Figure 6. The predicted elastic strain distribution from the eigenstrain distribution in the M(T) specimen was again in excellent agreement with the experimental results. This verifies the assumption of a continuously processed body.

Crack extension was modelled by removing the boundary conditions along the symmetry line. In order to be able to compare with the experiment results, the stresses were averaged over the measured gauge volume. The stresses averaged over the gauge volume converged readily despite the stress concentration at the crack tip.

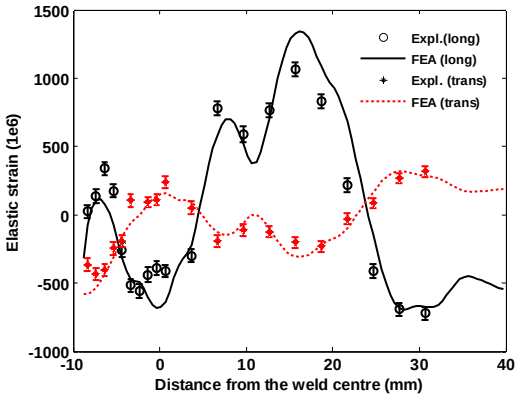

Figure 6 Experimentally determined and predicted residual elastic strains in the CT specimen from the eigenstrain distribution in the M(T) specimen (in un-fatigued condition)

The predicted residual stresses (using the initial stresses or eigenstrain distribution in the un-cracked M(T) at 12 mm crack length for the M(T) specimen and at 29 mm fatigue crack growth for the CT specimen are shown in Figure 4. The predicted elastic re-distribution with crack growth was in reasonably good correlation with the experimental results and hence it can be concluded that to a first approximation, the evolution of weld residual stresses is principally governed by elastic re-distribution [6, 7].

4 PREDICTING THE EFFECT OF RESIDUAL STRESSES ON FCG BEHAVIOUR

In section 4.1 the *R*-ratio and effective stress intensity factor range are computed using the residual stress and crack closure approach, respectively. In section 4.2 these values are used to predict the fatigue crack growth rates using an empirical fatigue crack growth law.

4.1 The effective stress intensity factor range and R-ratios

There are two different approaches that are often used to account for residual stresses in prediction of their effect on fatigue crack growth rates. These are superposition [15] and the effective stress intensity factor range (ΔK_{eff}) approach first introduced by Elber [16]. The stress intensity factors were in both cases computed using the J-Integral [17].

Superposition involves computation of the effect of the residual stresses on the 'actual' elastic stress intensity range at the crack tip (i.e. the residual stress intensity factor can be added to the applied stresses intensity factor). For the CT specimen strict superposition was not valid due to non-linear contact conditions between the crack faces [8]. Hence the stress intensity factor was calculated at both P_{max} and P_{min} for this specimen. The stress intensity range (ΔK) and stress ratio (R) was then computed as:

$$\Delta K = K_{\max} - K_{\min}, \quad R = \frac{K_{\min}}{K_{\max}}, \quad K_{\min} \geq 0 \tag{4}$$

$$\Delta K = K_{\max}, \quad R = 0, \quad K_{\min} < 0 \tag{5}$$

In the effective stress intensity factor approach (ΔK_{eff}), the crack opening stress intensity factor (K_{op}) is measured and the SIF range at which crack growth occurs (ΔK_{eff}) is computed as follows:

$$\Delta K_{eff} = K_{applied/\max} - K_{op} \tag{6}$$

4.2 Prediction of the fatigue crack growth rates

The NASGRO equation which is effectively a empirical Paris type relation in a sigmoid form was used to predict the changes in crack growth rates arising from the changes in R ratio caused by the varying K_{resid} and calculated using the residual stress (equations 4 and 5):

$$\frac{da}{dN} = \left[C\left(\frac{1-f}{1-R}\right)\Delta K \right]^n \frac{\left(1 - \frac{\Delta K_{th}}{\Delta K}\right)^p}{\left(1 - \frac{K_{\max}}{K_{crit}}\right)^q} \tag{7}$$

where C, n, p, q and f are empirical material parameters. The relevant material constants for 2024-T351 are available in the AFGROW database [18]. For the crack closure approach (equation 6) closure free fatigue crack growth data (R=0.7) was used to predict the effect of the residual stresses via experimental measurements of K_{op} [5].

The predicted results for the M(T) are compared with experimental results in Figure 2a (residual stress approach) and Figure 2b (crack closure approach). There is a good correlation between the experimental results using the residual stress approach for ΔK=6 and 11. For ΔK=15 the prediction was very conservative as the rate in this case was not significantly accelerated compared with the parent plate. For the crack closure approach the results were highly non-conservative for the lower stress intensity factor range but a good prediction was obtained at ΔK=15. As expected, excellent prediction of the rate in the parent plate tested at ΔK=11 was found.

The predicted rates for the CT specimen (Figure 3a) at the lower stress intensity ranges were in reasonable correlation with the experimental results using the residual stress approach. Excellent prediction was found for the specimen tested at ΔK=15. A reasonable prediction was also found for this case using the crack closure approach.

The two approaches to crack growth rate prediction are largely equivalent, as the crack growth rates derived during the K_{resid} technique are those predicted by the NASGROW equation for the local crack tip R ratio. The equation constants and its form are based on experimentally measured crack growth data for parent 2024 plate at different mean stresses. In turn, these measured growth rates reflect the effects of crack closure and other parameters operating in those test conditions. The crack closure behaviour is of course measured directly

in the ΔK_{eff} approach and is used to calculate the resultant growth rate. The K_{resid} approach has the advantage that it will reflect the possible influence of R ratio parameters influencing crack growth rates which are not associated with crack closure.

5 CONCLUDING REMARKS AND FUTURE WORK

Initial residual stresses in a welded plate were found to re-distribute with crack growth and the distribution is very different in the M(T) and CT specimens. More importantly the residual stresses have accelerated fatigue crack growth rate in the M(T) specimen whereas they decelerated the growth rate in the CT sample. Thus, fatigue crack growth rates obtained from laboratory specimens, of which the exact residual stress field is not known, may be misleading. It is critical that such factors are taken into account when designing damage tolerant aerospace structures based on laboratory specimen data.

The effect of the residual stress on the R-ratio (K_{min}/K_{max}) and ΔK_{eff} was computed for both specimen geometries using both the residual stress and crack closure approaches. The calculated stress intensity factor range or effective stress intensity factor range was then used to predict the fatigue crack growth rate employing an empirical fatigue crack growth law. The predicted FCGR in the welded M(T) specimens agreed well with the tests conducted at the lower load levels using the residual stress approach. There was however a dip in the experimental FCGR data at about 10 mm which wasn't picked up by the model. This might be due the micro structural changes in the transition between the HAZ and the parent material (Figure 3b) which are not included in the model at this time. The largest discrepancy between the experimental results and the predictions was found for the M(T) specimen at lower loads using the crack closure approach. For an open crack or a very small closure this might give misleading results as any non-linearity might be interpreted as crack opening. At the highest loads, a conservative prediction was obtained using the residual stress approach. This might be due to significant residual stress relaxation caused by gross plastic effects at this level of load. A good prediction was in this case obtained using the crack closure approach. For the CT specimen, both the experimental results and both sets of predictions were in good agreement.

To obtain better agreement models that incorporate both residual stress and crack closure methods may be needed. The good prediction of residual stress re-distribution achieved in this study by elastic redistribution may be the result of growing the crack at a constant stress intensity range, which was achieved by reducing the applied stress with increasing crack length. To assess this assumption future work could be to measure and model the evolution of residual stresses in specimens loaded at constant amplitude load. This scenario is closer to the situations in practice and will allow assessment of the affect of plastic relaxation of the residual stress field on crack growth behaviour.

REFERENCES

[1] UK DTI Aerospace innovation growth team report June 2003.
[2] J.F. Throop and H.S Reemsnyder, ASTM 04-776000-30, 1981.
[3] M.E. Fitzpatrick and L. Edwards, "Fatigue Crack / Residual Stress Field Interactions and

their Implications for Damage Tolerant Design", *J. Mat. Eng. & Perf.,* **7**, 190-198 (1998)
[4] L. Edwards, M.E. Fitzpatrick, P.E. Irving, I. Sinclair, X. Zhang and D. Yapp, "An integrated approach to the determination and consequences of residual stress on the fatigue performance of welded aircraft structures", *J. ASTM Int.*, **3**, JAI12547, doi: 10.1520/JAI12547 (2006).
[5] J. Brouard, J. Lin J and PE Irving, "Effects of residual stress and fatigue crack closure during fatigue crack growth in welded 2024 aluminium", Proceedings of Fatigue 2006, Atlanta, USA, June 2006.
[6] C.D.M. Liljedahl, J.F. Tan, O. Zanellato, S. Ganguly, M.E. Fitzpatrick and L. Edwards, "Evolution of residual stresses with fatigue loading and subsequent crack growth in VPPA welded aluminium alloy MT specimen", Submitted.
[7] C.D.M. Liljedahl, O. Zanellato, S. Ganguly, M.E. Fitzpatrick and L. Edwards, "Evolution of residual stresses with fatigue loading and subsequent crack growth in a VPPA welded aluminium alloy CT specimen", Submitted.
[8] C.D.M. Liljedahl, J.F. Tan, O. Zanellato, S. Ganguly, M.E. Fitzpatrick and L. Edwards, "The effect of the residual stresses on the FCGR in a MT and CT specimen sectioned from a welded plate", Submitted.
[9] Santisteban, JR, Daymond MR, James JA and Edwards L, "ENGIN-X: a third generation neutron strain scanner", *J. Appl. Cryst.*, **39**, 812-825 (2006).
[10] T. Tsakalakos, M.C. Croft, N.M. Jisrawi, R.L. Holtz and Z. Zhong, "Measurment of residual stress distributions by energy dispersive X-ray diffraction syncrotron radiation", Internacional Offshore and Polar Engineering Conference, San Francisco, California, USA, May 2006.
[11] M. Croft, Z. Zhong, N. Jisrawi, I. Zakharchenko, R.L. Holtz, J. Skaritka, T. Fast, K. Sadananda, M. Lakshimpathy and T. Tsakalakos, "Strain profiling of fatigue crack overload effects using energy dispersive X-ray diffraction", Int. J. Fatigue, **27**, 1408-1419 (2005).
[12] M.R. Hill, "Modelling of residual stress effects using eigenstrain", 10th International Conference on Fracture, Oahu, Hawaii, December 2001.
[13] A.T. DeWald and M.R. Hill, "Multi-axial contour method for mapping residual stresses in continuously processes bodies", *Exp. Mech.*, **46**, 473-490 (2006).
[14] ABAQUS Version 6.5, Hibbitt, Karlsson & Sorensen, Inc., 2005.
[15] P. Parker,"Linear elatic fracture mechanics and fatigue crack growth – residual stress effects", Sagamore Army Materials Research Conference proceedings, 1982.
[16] W. Elber, "The significance of fatigue crack closure, in Damage Tolerance in Aircraft Structures", ASTM STP, **486**, 230-242 (1971).
[17] J. Rice, "A path independent integral and approximate analysis of strain concentration and cracks", J. Appl. Mech., **35**, 379-387 (1968).
[18] J.A. Harter, AFGROW Users Guide and Technical Manual, AFRL-VA-WP-TR-2004, 2004.